Surface atomic structure of reconstructed $VC_{0.8}(111)$ studied with scanning tunneling microscopy

M. Hammar, C. Törnevik, J. Rundgren, Y. Gauthier,* and S. A. Flodström
Department of Physics, Materials Science, Royal Institute of Technology, S-100 44 Stockholm, Sweden

K. L. Håkansson and L. I. Johansson
Department of Physics and Measurement Technology, Linköping University, S-581 83 Linköping, Sweden

J. Häglund
Department of Theoretical Physics, Royal Institute of Technology, S-100 44 Stockholm, Sweden
(Received 12 July 1991)

Scanning tunneling microscopy has been performed on the reconstructed polar surface of substoichiometric $VC_{0.80}(111)$. A mixture of (8×1) and $(\sqrt{3}\times\sqrt{3})R30°$ reconstructed areas was found. The (8×1) periodicity could be determined to be the result of a square-lattice surface layer superimposed on the hexagonal substrate. As this square lattice must have its origin in strong and directed in-plane bonds with the relatively large length of about 2.9 Å, it can be deduced to consist of vanadium atoms. Lateral positions of these vanadium surface atoms with respect to the substrate are suggested from the measured surface corrugation. The $(\sqrt{3}\times\sqrt{3})R30°$ structure was found in small triangular areas which can, due to the measured step heights between the two reconstructions, be believed to be carbon terminated. The occurrence of a reconstructed surface with a reduced atomic concentration is in contrast to what is known for TiC(111) and NbC(111), both having stable (1×1) surfaces. A qualitative explanation for this difference is suggested.

I. INTRODUCTION

Vanadium carbide has properties that are typical of an important group of transition-metal carbides and nitrides (TMCN's) which solidify in the sodium chloride structure. These materials possess metallic conductivity, ultrahardness, and extremely high melting points, properties that are related to their unusual combination of binding mechanisms: a mixture of covalent, ionic, and metallic bonding.[1] They seldom appear in the stoichiometric form but most often contain vacancies in the nonmetal lattice sites with a wide range of compositions. As these vacancies may strongly affect the macroscopic properties, their distribution and influence have been studied by several researchers. For instance, the existence of a long-period superlattice (LPS) in VC_{1-x}, with $1-x$ in the range 0.75–0.88, has been observed using transmission electron microscopy.[2] The LPS, which was interpreted as a bulk vacancy ordering, was created above a critical temperature of about 1000 °C and observed on all low-index surfaces. With low-energy electron diffraction (LEED), no superstructures were observed on the (100) and (110) faces of a $VC_{0.80}$ sample,[3,4] but a three-domain (8×1) pattern was reported to appear after heat treatment above 1000 °C on the (111) surface.[5] This surface is polar, which means that pure vanadium layers alternate with pure carbon layers in the ⟨111⟩ directions, and hence the ideal surface should be either vanadium or carbon terminated.

Among the (111) surfaces of these materials only a few have been studied. Using different techniques such as electron spectroscopy and ion scattering spectroscopy, $TiC_{1-x}(111)$ (Refs. 6–10) and $NbC_{1-x}(111)$,[11,12] which both have stable (1×1) surfaces, have been found to be metal terminated. A recent LEED study[13] yielded the same result for the metastable surface of $VC_{0.80}(111)(1\times1)$.

In this study we have used scanning tunneling microscopy (STM) in order to clarify the atomic structure of the reconstructed $VC_{0.80}(111)$ surface. We also suggest a qualitative explanation for differences in structural stability of the (111) surfaces between various TMCN's.

II. EXPERIMENTAL DETAILS

The experiments were performed in an ultrahigh-vacuum (UHV) system with a base pressure better than 1×10^{-10} Torr. The STM[14] is housed in a separate chamber into which samples and tips can be transferred from a preparation and analysis chamber, which *inter alia* includes equipment for LEED. Growth and preparation of the sample, a $VC_{0.80}$ single crystal with a mirror-polished (111) face, are described elsewhere.[13,15] In vacuum the sample was cleaned and recrystallized by means of Ar^+-ion sputtering, 10 min each at 1.5 and 0.5 kV, and electron bombardment annealing. The temperatures were measured with a pyrometer and the annealing times were kept constant to 15 min. During the course of the STM experiments the sample was kept clean by means of flash heatings to above 1000 °C every sixth hour.

Heat treatment in the temperature range 700–900 °C resulted in a sharp (1×1) LEED pattern. Above 900 °C the onset of a phase transformation towards an (8×1)

reconstruction was observed. This was fully accomplished at about 1000 °C, above which a distinct LEED pattern was obtained. In some sample areas all three domains of the reconstruction could clearly be seen, whereas in others only one domain, or sometimes two, was visible. The (8×1) reconstruction was preserved after additional heat treatments at lower temperatures and the surface had to be sputtered in order to obtain the (1×1) structure again. After annealing at temperatures intermediate to those giving rise to the well-defined (1×1) and (8×1) surface structures, very weak traces of a $(\sqrt{3}\times\sqrt{3})R30°$ reconstruction were occasionally seen. However, the related LEED spots were not present at the final step where the (8×1) reconstructed surface was investigated with the STM.

The STM images were obtained with a tunneling current of 1 nA and the sample biased to -5 mV with respect to the electrochemically etched tungsten tips. However, within ±0.5 V and 0.1–2 nA the voltage and current settings were not critical and a reversal of the sign did not cause any noticeable influence on the images.

III. RESULTS AND DISCUSSION

A representative large area image of the surface, which was always found to be well ordered and remarkably flat, is presented in Fig. 1. The (8×1) periodicity appears in the broad bands traveling over the surface. These bands have mutual angles of 120°, in agreement with the LEED pattern, and define small intermediate triangular areas as they intersect with each other. It can be seen that the reconstruction has a preferential orientation along the steps. This behavior is more pronounced in regions which are slightly tilted with respect to the crystallographic (111) plane with a high density of parallel steps. In such stepped regions, which were found to dominate the surface, only one (8×1) domain, parallel to the steps, was present, whereas the triangular areas were almost absent. In flatter regions, however, the triangles were found to occupy a larger portion of the surface, in some cases up to 50%. The alignment of the (8×1) reconstruction with steps is also recognized at the boundaries to the triangular areas, each triangle being isosceles with legs in $\langle 1\bar{1}0\rangle$-type directions. The in-plane boundaries between different (8×1) domains, e.g., between the domains which surround the triangular areas, are always disordered reflecting an obvious geometrical mismatch in the atomic registry. As a result, there are always disordered lines propagating in some random direction from each corner of the triangles. An example is seen in the middle top part of Fig. 2.

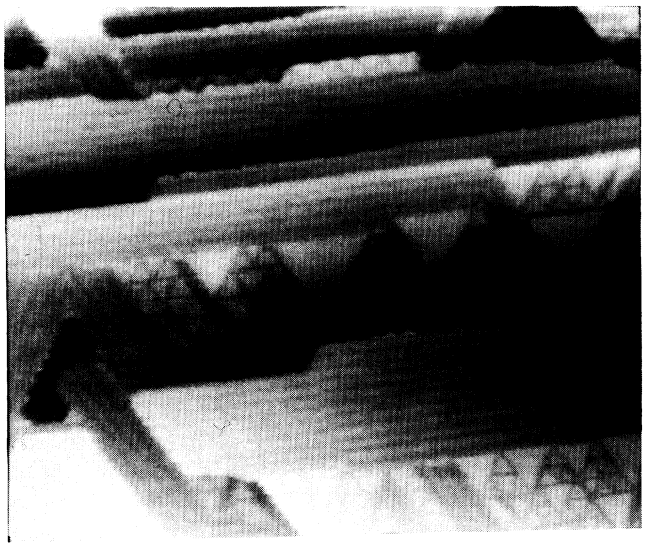

FIG. 1. A 1000×860 Å^2 STM image of the VC(111) surface. It can be seen that the (8×1) reconstruction has a preferential orientation with the steps, causing the phase with a horizontal orientation to dominate the image. The flat triangular areas possess a $(\sqrt{3}\times\sqrt{3})$ surface reconstruction which is not resolved here. The full gray scale range corresponds to a total height difference of 14 Å.

A closer examination of the steps between adjacent domains reveals some interesting features. The height difference between neighboring (8×1) reconstructed regions was measured to be 2.4 ± 0.1 Å or multiples thereof. Such step heights are to be expected if the surface is either vanadium or carbon terminated, in agreement with a double-layer distance of $2d_{111}=2.39$ Å.[16] However, the steps between the (8×1) reconstructed bands and the triangular areas were found to be 1.1 ± 0.1 Å, suggesting a single-layer distance. One possible conclusion is that the surface has a mixed termination with vanadium in the bands and carbon in the triangles, or vice versa.

The high-resolution image in Fig. 2 reveals the origin of the (8×1) reconstruction. It is due to a rectangular surface layer, corresponding to a coverage of $\frac{7}{8}$ ML, superimposed on the hexagonal substrate. The periodicity of the surface atoms is a and $(48/49)^{1/2}a$ in the $\langle 1\bar{1}0\rangle$ and $\langle 11\bar{2}\rangle$ directions, respectively, where a is the surface lattice parameter. Figure 3(a) is a partial magnification of a few unit cells in Fig. 2 and is intended for comparison with the simulated images in Figs. 3(b)–3(d), each of which corresponds to a specific structure model. From LEED intensity measurements[17] it is known that the reconstruction is symmetric in $\langle 1\bar{1}0\rangle$-type directions, whereas no such conclusion could be made about $\langle 11\bar{2}\rangle$ directions. This means that the surface atoms are determined to be distributed along lines in $\langle 11\bar{2}\rangle$-type directions, which pass directly over second-layer atoms. To establish the positions along those lines, the surface corrugation has to be examined in detail. In the lower parts of Figs. 3(b)–3(d), three possible cases are shown by ball models in which the topmost vanadium (an assumption which will be argued for below) atoms are arranged upon an undisturbed carbon layer according to the observed lateral interdistances and the known vanadium-carbon distance in the bulk under the assumption that a true hollow, bridge, or top position is occupied. The simulated images in the top parts of Figs. 3(b)–3(d) are due to the atomic charge superposition method described by Tersoff and Hamann.[18] Here, the STM corrugation is approximated by a surface of constant charge density. To calcu-

FIG. 2. A 105×35 Å^2 high-resolution image of the (8×1) reconstruction. It can clearly be seen that the surface layer has a square symmetry. The height difference between the highest and lowest atom in the (8×1) unit cell is about 0.6 Å. Note the disordered boundary between the (8×1) domains.

late this quantity, each atom on the surface has been assigned a spherically symmetric and exponentially decaying charge density, which then can be added at each point over the surface. The inverse decay length is calculated as $\kappa=\hbar^{-1}(8m\phi)^{1/2}$, where ϕ is the work function. Due to a lack of information on this (less critical) value for VC(111), we have used the work function for TiC(111), 4.7 eV.[9] The tip-surface distance has finally been chosen so as to optimize the agreement with the experimental image. This optimization required a rather narrow tip-surface distance, as measured from the center of the tip atom to the center of the surface atoms, of about 2.5 Å, probably reflecting the fact that the actual tip and surface wave functions have *d* rather than *s* character.[19] It is clear from inspection that the best fit is obtained if a true top position is assumed, as in Fig. 3(d). Among the three models, only this configuration satisfactorily reflects the observed symmetry in the images. The most obvious feature to focus on here is the two lowest and equally depressed atoms which are identified as Nos. 6 and 7 from the left in Fig. 3(d), but that have no resemblance in Figs. 3(b) or 3(c). Some local deviation from the model due to noise and irregularities is present, but the general trend is very clear and also the corrugation of the remaining five atoms in the sequence is well reproduced. It can be argued that it is not possible to distinguish between positions close to the precise top site. However, the corrugation is very sensitive to lateral movements and the observed symmetry in the images guarantees an atomic configuration close to the one shown in Fig. 3(d). Note that only 0.24 and 0.12 Å separate the top from the hollow and bridge cases, respectively, limiting the total lateral translation between equivalent points to 0.36 Å. The height difference between the extreme atomic positions (top and near hollow sites, respectively) was measured to be around 0.6 Å, in good agreement with the ball model for the top case, which predicts 0.59 Å for this difference.

The triangular areas have a completely different surface structure with a $(\sqrt{3}\times\sqrt{3})R30°$ reconstruction being found; see Fig. 4. The measured corrugation in the corresponding STM images is much smaller than in the (8×1) case, the height difference within the surface unit cell is only 0.15 Å and the individual atoms are not well resolved. Anyway, a honeycomb pattern of atoms surrounding the hexagonally distributed hollows are recognized, and based on the STM images we believe that the atomic configuration is as indicated in Fig. 4 with one atom in each corner of the outlined hexagons. This would then correspond to a surface coverage of $\frac{2}{3}$ ML, i.e., one-third of the carbon atoms are missing as compared with an ideal carbon-terminated surface. It is interesting to note that this superstructure was not detected by the LEED observation prior to this STM investigation. Presumably, the reason for this was that the triangular areas occupied a too-small portion of the surface to contribute to the LEED pattern, which averages over a rather macroscopic area. In spite of this, they were readily found with the STM. However, as previously mentioned, this reconstruction was observed after annealing at intermediate temperatures, corresponding to the transition between the (1×1) and (8×1) phases. It was also observed on the same sample, in the same temperature range but in a different vacuum system, during a dynamical LEED analysis.[17] Also in that study, the related spots were found to be very weak, more than an order of magnitude weaker than the other spots, and to vanish completely after the high-temperature annealing leading to the sharp (8×1) pattern.

There are several possibilities for how the (8×1) reconstructed bands and the $(\sqrt{3}\times\sqrt{3})R30°$ reconstructed triangles are terminated, i.e., if they have vanadium or carbon or perhaps a mixture thereof in the uppermost layer. This can be discussed as follows.

Vanadium carbide has, as stated above, the sodium chloride structure. In the case of $VC_{0.80}$ the lattice parameter is approximately 4.15 Å,[16] which corresponds to a nearest-neighbor distance in the ideal (111) surface of 2.93 Å. This means that the size of the rectangles in the (8×1) reconstruction, which must have its origin in strong and directed bondings within the surface layer, is 2.93×2.90 Å^2. As a consequence of the carbon covalent radii being about 0.77 Å, such large distances rule out the possibility of carbon termination so it can be concluded that the surface layer consists of vanadium atoms in this case. This conclusion makes, as previously mentioned, a carbon termination in the triangular areas likely.

From LEED and Auger-electron-spectroscopy measurements, Bradshaw *et al.*[17] could conclude the coex-

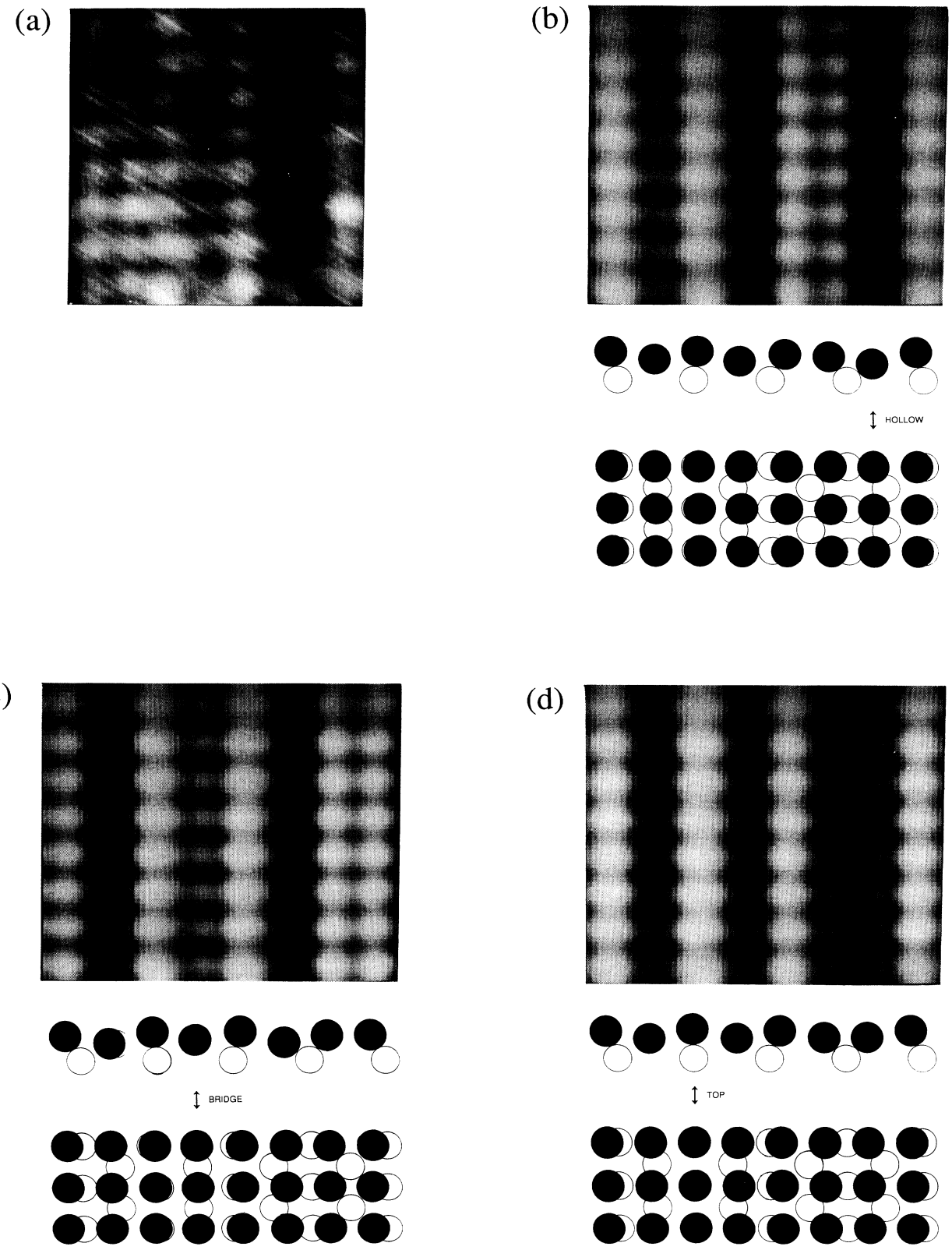

FIG. 3. (a) A section from Fig. 2 to be compared with the simulated images in (b)–(d). (b) A simulated image corresponding to the case where one true hollow site is occupied as is shown by the ball model. (c) Same as (b) but corresponding to a true bridge site. (d) Same as (b) but corresponding to a true top site. The leftmost and rightmost atomic rows in these images and ball models are identical. The horizontal magnification is somewhat larger than the vertical in the simulated images, leading to their slight rectangular shape.

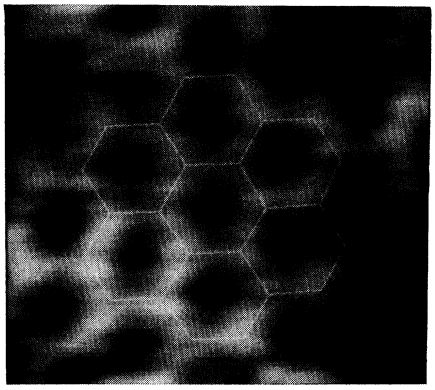

FIG. 4. 27×22 Å^2 image showing the $(\sqrt{3}\times\sqrt{3})$ structure within a triangular area of the kind seen in Fig. 2. The atomic positions are indicated by the outlined hexagons and correspond to a surface coverage of $\frac{2}{3}$ ML. Note that the lines in the hexagons do not symbolize chemical bonds. The total height difference in the image is only 0.2 Å.

istence of TiC(111)(1×1)-Ti and TiC(111)(1×1)-C domains after high-temperature annealings, i.e., a surface composition similar to the one here proposed for VC, a mixed termination of metal and carbon atoms, but with a different surface structure also for the carbon-terminated areas.

At this point a comparison with the metal-terminated TiC(111)(1×1) and NbC(111)(1×1) surfaces is worthwhile. In the former case, Zaima *et al.*[9] argued for an enhanced metallic bonding at the surface. They based this argument on the observation that the TiC(111) surface seems to be thermodynamically stable in comparison to the TiC(110) face, which forms facets after heat treatment. This is in contrast to what would be expected from a simple broken-bond model for the surface free energy, at least if it is assumed that the stability of the compound originates mainly from strong covalent metal-nonmetal bondings as has been suggested, e.g., in Refs. 20 and 21. Hence, these authors draw the conclusion that the stability of the TiC(111) surface must be explained in terms of atomic or electronic relaxation. They also pointed out that the surface atomic structure is similar to the one on Ti(0001) and equals the one on a fcc(111) surface, which is the most stable in fcc metals. Consequently, an enhancement of the Ti-Ti bondings should stabilize the surface. This was also in agreement with an observed similarity in the electronic structure of TiC(111) and Ti(0001).[7]

Indeed, an enhanced surface metallic bonding seems to be the case on VC(111)(8×1). The surface layer has a structure very similar to the (100) surface of pure vanadium, which has a bcc lattice with the parameter 3.03 Å. However, this is not the most stable surface of a metallic bcc crystal, nor does it equal the (111) face of a fcc lattice, and so it is somewhat inconsistent with the discussion of Zaima *et al.*,[9] which hence cannot be applied here. Furthermore, it is not clear which contribution to the chemical bonding in these compounds is the most important, the transition-metal *d-d* interaction or the hybridization between the metal *d* shell and the light-element *sp* shell.[22] Thus, any conclusions involving broken bonds on the surface, like the one mentioned above, must be handled with great care.

A complete theoretical understanding of why the VC(111) surface rearranges to the structure described in this paper instead of remaining unchanged or taking a different structure would involve a discussion of subtle differences in energy contributions from competing surface structures. In view of the difficulties of even determining stable bulk lattice configurations for the elements, it is likely that a theoretical prediction of the surface structure of a transition-metal carbide would be erroneous. However, we here suggest a qualitative explanation of why the (111) surface of VC chooses a reconstruction with a lower concentration of atoms, while the (111) surfaces of the neighboring carbides, TiC and NbC, remain stable in their bulk positions. The fact that VC and NbC have different surface structures is particularly interesting since one naively could expect that these two compounds, due to their closely related electronic configurations, should have similar stability properties. An extensive analysis of the structural stability of all carbides and nitrides in the NaCl structure of the 3*d* and 4*d* transition metals has been carried out in Refs. 23 and 24, using both theoretical methods and an analysis of thermodynamic information. The results of these works are displayed in Fig. 5, where the cohesive energy per atom ($E_{\rm coh}$) is plotted for carbides in the beginning of the 3*d* and 4*d* series. A well-pronounced maximum in the stability curve for the 3*d* series is obtained for TiC. The fact that this carbide is particularly stable can be qualitatively understood from simple band-filling considerations.[25] In the 4*d* series the corresponding maximum lies on NbC and not on ZrC, which might have been suggested from a naive rigid-band model.

The obvious application to the surface-stability problem is now to argue that a compound with maximal structural stability in the bulk lattice configuration, i.e., with maximal cohesive energy ($E_{\rm coh}$), is less likely to rearrange its surface atoms, while a compound lying on

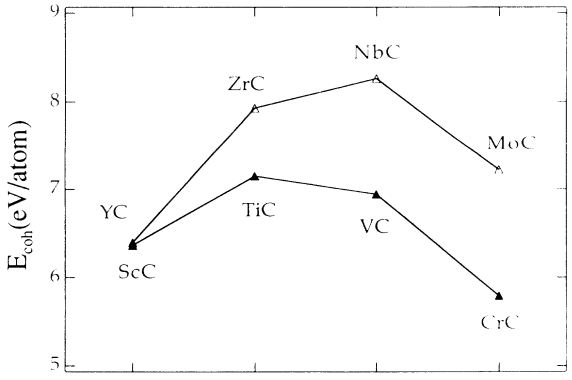

FIG. 5. Cohesive energies for NaCl-structure carbides in the 3*d* and 4*d* transition-metal series.

the "slope" of the stability curve (Fig. 5) probably can gain energy by a redistribution. For compounds on the "uphill" side of the curve it would be favorable to increase the number of valence electrons in the valence band, while compounds on the "downhill" side of the maximum in E_{coh} would gain structural energy by decreasing the concentration of atoms at the surface. This argument agrees well with the fact that the surface layer of V and C atoms contains $\frac{7}{8}$ and $\frac{2}{3}$ of the normal V and C concentration in the (111) layer of VC. A similar prediction can, of course, also be made for the nitride surface structures in the 3*d* and 4*d* series, where the stability curve maxima is observed on ScN and NbN.[19,24] Unfortunately, none of the (111) nitride surfaces in the series have been examined in the literature and the only relevant surfaces to test these predictions against are TiC(111) and NbC(111).

It has been suggested that a surface structure with a reduced atomic concentration can also be understood in terms of the compensational charge required on a polar surface.[26] This effect, however, can hardly explain the difference in surface structures between compounds of metals of the same group in the Periodic Table, e.g., VC(111) and NbC(111).

IV. SUMMARY

The reconstructed polar surface of substoichiometric $VC_{0.80}(111)$ has been examined using STM under UHV conditions. Two different surface reconstructions were found. One, which has an (8×1) periodicity with three possible orientations on the surface, was interpreted as a square lattice of surface vanadium atoms on top of the hexagonal substrate. From a close examination of the surface corrugation, the lateral positions of the surface layer vanadium atoms could be suggested. The other reconstruction has a $(\sqrt{3}\times\sqrt{3})R30°$ structure and appears in small triangular areas. Step heights to adjacent (8×1) domains suggest these areas to be carbon terminated. Finally, a qualitative explanation for the difference in the observed surface geometries on various transition-metal compounds was proposed.

ACKNOWLEDGMENTS

This work was performed with financial support from the Swedish Natural Science Research Council (NFR) and the K. and A. Wallenberg Foundation.

*Permanent address: Laboratoire de Spectrométrie Physique, Université Joseph Fourier, Boîte Postale 87, 38402 Saint Martin d'Héres, France.

[1]L. E Toht, *Transition Metal Carbides and Nitrides* (Academic, New York, 1971).

[2]See, e.g., T. Epicier, M. G. Blanchin, P. Ferret, and G. Fuchs, Philos. Mag. **59**, 885 (1989), and references therein.

[3]P. A. P. Lindberg, L. I. Johansson, and A. N. Christensen, Surf. Sci. **192**, 353 (1987).

[4]P. A. P. Lindberg, L. I. Johansson, and A. N. Christensen, Z. Phys. B **69**, 521 (1988).

[5]P. L. Wincott, P. A. P. Lindberg, and L. I. Johansson (unpublished).

[6]J. H. Weaver, A. M. Bradshaw, J. F. van der Veen, F. J. Himpsel, D. E. Eastman, and C. Politis, Phys. Rev. B **22**, 4921 (1980).

[7]A. M. Bradshaw, J. F. van der Veen, F. J. Himpsel, and D. E. Eastman, Solid State Commun. **37**, 37 (1980).

[8]C. Oshima, M. Aono, S. Otani, and Y. Ishizawa, Solid State Commun. **48**, 911 (1983).

[9]S. Zaima, Y. Shibata, H. Adachi, C. Oshima, S. Otani, M. Aono, and Y. Ishizawa, Surf. Sci. **157**, 380 (1985).

[10]R. Souda, C. Oshima, S. Otani, Y. Ishizawa, and M. Aono, Surf. Sci. **199**, 154 (1988).

[11]I. Kojima, M. Orita, E. Miyazaki, and S. Otani, Surf. Sci. **160**, 153 (1985).

[12]E. Edamoto, T. Anazawa, E. Shiobara, M. Hatta, E. Miyazaki, H. Kato, and S. Otani, Phys. Rev. B **43**, 3871 (1991).

[13]J. Rundgren, Y. Gauthier, R. Bandoing-Savois, Y. Joly, and L. I. Johansson, Phys. Rev. B (to be published).

[14]Omicron Vakummphysik GmbH, Taunusstein, West Germany.

[15]A. N. Christensen, J. Cryst. Growth **33**, 99 (1976).

[16]The lattice parameter, 4.147 Å for $VC_{0.80}$, was obtained from a linear interpolation of data given in J. P. Landesman, G. Tréglia, P. Turchi, and F. Ducastelle, J. Phys. **46**, 1001 (1985).

[17]Y. Gauthier and R. Baudoing-Savois (unpublished).

[18]J. Tersoff and D. R. Hamann, Phys. Rev. B **31**, 805 (1985).

[19]For a discussion, see C. J. Chen, Phys. Rev. Lett. **65**, 448 (1990).

[20]A. Neckel, P. Rastl, R. Eibler, P. Weinberger, and K. Schwarz, J. Phys. C **9**, 579 (1976).

[21]W. Weber, Phys. Rev. B **8**, 5082 (1973).

[22]See, e.g., C. D. Gelatt, Jr., A. R. Williams, and V. L. Moruzzi, Phys. Rev. B **27**, 2005 (1983).

[23]J. Häglund, G. Grimvall, T. Jarlborg, and A. Fernández Guillermet, Phys. Rev. B **43**, 14 400 (1991).

[24]A. Fernández Guillermet, J. Häglund, and G. Grimvall (unpublished).

[25]A. Fernández Guillermet and G. Grimvall, Phys. Rev. B **40**, 10 582 (1989).

[26]R. W. Nosker, P. Mark, and J. D. Levine, Surf. Sci. **19**, 291 (1970).

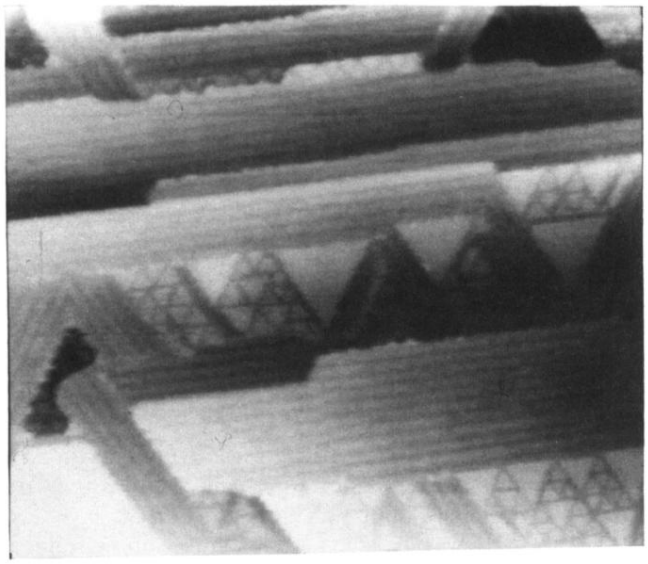

FIG. 1. A 1000×860 Å^2 STM image of the VC(111) surface. It can be seen that the (8×1) reconstruction has a preferential orientation with the steps, causing the phase with a horizontal orientation to dominate the image. The flat triangular areas possess a $(\sqrt{3} \times \sqrt{3})$ surface reconstruction which is not resolved here. The full gray scale range corresponds to a total height difference of 14 Å.

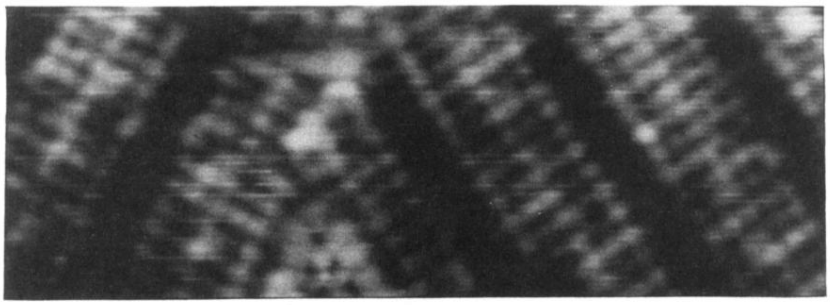

FIG. 2. A 105×35 Å^2 high-resolution image of the (8×1) reconstruction. It can clearly be seen that the surface layer has a square symmetry. The height difference between the highest and lowest atom in the (8×1) unit cell is about 0.6 Å. Note the disordered boundary between the (8×1) domains.

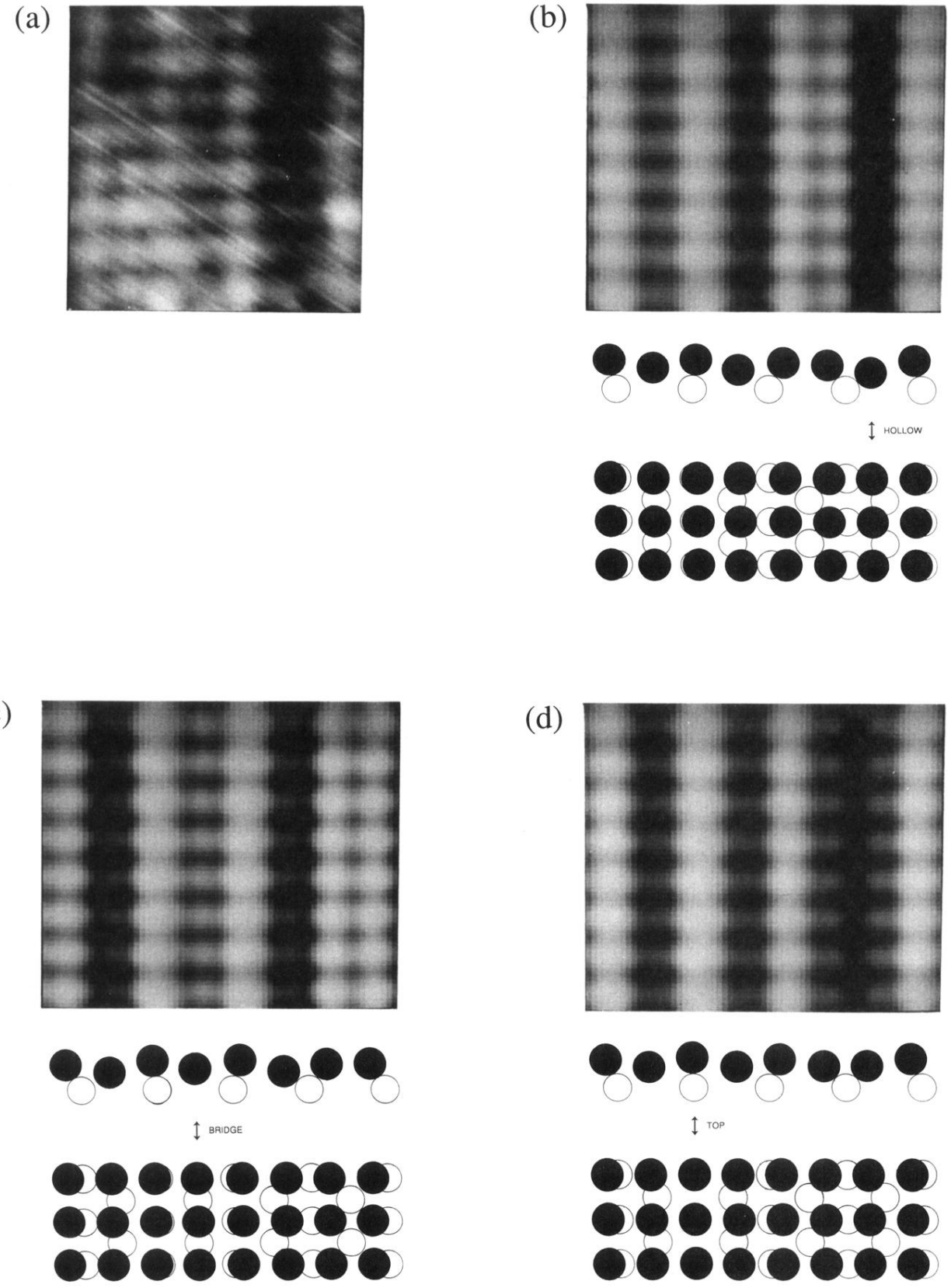

FIG. 3. (a) A section from Fig. 2 to be compared with the simulated images in (b)–(d). (b) A simulated image corresponding to the case where one true hollow site is occupied as is shown by the ball model. (c) Same as (b) but corresponding to a true bridge site. (d) Same as (b) but corresponding to a true top site. The leftmost and rightmost atomic rows in these images and ball models are identical. The horizontal magnification is somewhat larger than the vertical in the simulated images, leading to their slight rectangular shape.

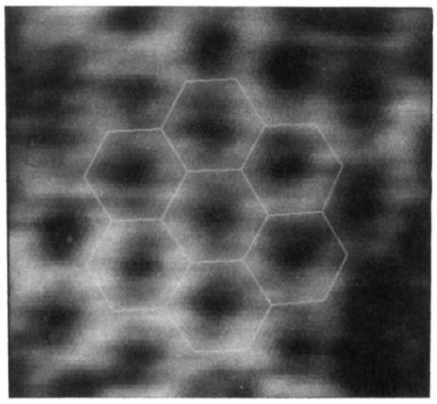

FIG. 4. 27×22 Å^2 image showing the $(\sqrt{3} \times \sqrt{3})$ structure within a triangular area of the kind seen in Fig. 2. The atomic positions are indicated by the outlined hexagons and correspond to a surface coverage of $\frac{2}{3}$ ML. Note that the lines in the hexagons do not symbolize chemical bonds. The total height difference in the image is only 0.2 Å.